Nuclear Physics B299 (1988) 21–51
North-Holland, Amsterdam

HEAVY FLAVOUR PRODUCTION AT HERA

Gerhard A. SCHULER

Deutsches Elektronen-Synchrotron DESY, Hamburg, FR Germany

Received 16 September 1987

We present explicit formulae for the total differential cross sections of heavy flavour production at HERA including γ-Z^0 interference and W-exchange. We evaluate total top production rates and discuss theoretical uncertainties. Assuming an integrated luminosity of 100 pb^{-1} we estimate that a top quark mass up to 100 GeV can be probed.

1. Introduction

One of the main topics of forthcoming electron-proton colliders like HERA [1] is heavy flavour production. Production and decay of heavy fermions are ideal reactions to test the standard model [2]. In the electroweak sector they allow for a determination of, for example, the electroweak coupling constants, the Cabibbo-Kobayashi-Maskawa matrix elements and the quark masses. Furthermore, reactions involving heavy fermions are of importance in order to get information about possible extensions of the standard model. These reactions are in competition with reactions of models with supersymmetric particles or colour excited leptons and quarks [3].

In electron-proton colliders like HERA a heavy quark pair is created via the boson-gluon fusion mechanism [4] where the boson is either a W-boson, a photon, or a Z^0-boson. Total production rates will not only tell us which heavy quark mass is accessible at a given center of mass energy but also will give us information about the gluon structure function $G(x, Q^2)$ for small values of x. Furthermore, heavy flavour production will influence the value of $R_L = \sigma_L/\sigma_2$ as predicted by massless QCD. As a last point, the thresholds for heavy flavour productions lead to a power-like scaling violation [6]. This scaling violation is stronger than the logarithmic scaling violation [5] of massless QCD. Thus the latter can only be extracted after correcting for the scaling violation due to heavy flavours [6, 11].

There has been a great effort in the study of boson-gluon fusion* into heavy flavours. Several authors have calculated the process in the Weizsäcker-Williams

* The authors of [7, 8] also investigated higher order contributions. The corrections to $t\bar{t}$ production were found to be negligible. However, contributions coming from W production with subsequent decay into heavy flavours seem to produce rather large 20% (25%) corrections to the $\bar{t}b$ rate for $m_t = 50$ (70) GeV [11]. These calculations [8] were done in the Weizsäcker-Williams approximation and should be confirmed. We will neglect these contributions to the $\bar{t}b$ production in the following.

0550-3213/88/$03.50

approximation [7,9], for which Monte Carlo event generators even exist [12,19]. Numerical studies for charm production at fixed target experiments have been done as well [4]. Explicit formulae for the deep-inelastic structure functions F_i for heavy flavour production have existed for a long time [10]. They have been recently updated in refs. [11,12]*. Also some work has been done on the transverse momentum distribution of massive quarks [13].

However, in order to study the topology of heavy flavour production at HERA, the fully (five-fold) differential cross section is needed. Incorporating the fully differential cross section formula in a Monte Carlo event generator allows not only for an inclusion of the experimental setup but also for a study of the various dependences of the cross section and how far the theoretical input may be reconstructed. As a first step in this direction we present a calculation of heavy flavour production in electron-proton scattering, leading to an explicit formula for the total diffential cross section. We include both W-exchange and γ-Z^0 interference. Furthermore we allow for electron or positron scattering and include longitudinal polarization of the incoming lepton.

The organization of the paper is as follows: After defining the kinematical variables in sect. 2 and the electroweak contents in sect. 3, we give an explicit representation of the particle momenta and a discussion of the physical region boundaries in sect. 4. In sect. 5 we present the final formula for the total differential cross section. There we also perform the two integrations which can be done analytically and which yield the usual deep-inelastic structure functions F_1, F_2 and F_3. Sect. 6 contains a short description of the Weizsäcker-Williams approximation [WWA], whose applicability we investigate in the last section. There we present results for total rates of top production and discuss possible uncertainties of the results. Since the massive $O(\alpha_s)$ calculation contains additional kinematic and electroweak dependences compared to the massless case, we describe in the appendix the calculation of the matrix element in some length.

We find a top production cross section of about 0.02 pb^{-1} for $m_t = 100$ GeV. Assuming an integrated luminosity of 100 pb^{-1} and requiring at least 2 events for detection we estimate that a top mass up to 100 GeV should be observable at HERA.

2. Notation

We consider positron (electron) proton scattering into quarks of heavy flavours f and f':

$$e^{\pm}(l_e) + p(P) \to \ell(l) + q_f(p_f) + \bar{q}_{f'}(p_{f'}) + X \tag{1}$$

allowing for longitudinal polarized positrons (electrons). Here ℓ is either a positron (electron) or an (anti-) neutrino. We neglect the lepton masses whenever it is safe

* After submitting this work we learned that the heavy flavour structure functions have been considered recently also in [20].

(see below), thus:

$$l_e^2 = l^2 = 0, \tag{2}$$

whereas

$$P^2 = m_p^2, \qquad p_f^2 = m_f^2, \qquad p_{f'}^2 = m_{f'}^2. \tag{3}$$

Experimentally, no heavy quarks are seen within the proton-sea. The lowest order QCD realization of process (1) is assumed to happen via gluon emission out of the proton which in turn goes into a heavy quark-antiquark pair. We thus consider the subprocess:

$$e^{\pm}(l_e) + \text{gluon}(p) \to \ell(l) + q_f(p_f) + \bar{q}_{f'}(p_{f'}), \tag{4}$$

where we take the gluon to be on-shell ($p^2 = 0$).

To lowest order in the electroweak coupling α the process (4) happens via one-boson exchange, the boson being either the photon, the Z^0 or the W. This subprocess

$$\text{boson}(q) + \text{gluon}(p) \to q_f(p_f) + \bar{q}_{f'}(p_{f'}) \tag{5}$$

is the so-called boson-gluon fusion [4]. The momentum q of the boson is given by

$$q := l_e - l, \tag{6}$$

satisfying $p + q = p_f + p_{f'}$.

Let us define the following invariants (here $\hat{}$ denotes variables of the subsystem (5), e.g. $\hat{s}$ is the c.m.s. energy of (5)):

$$\begin{aligned} Q^2 &:= -q^2, \\ \hat{s} &:= s_{12} \equiv (p_f + p_{f'})^2, \\ \hat{t} &:= (p - p_f)^2, \\ \hat{u} &:= (p - p_{f'})^2, \end{aligned} \tag{7}$$

yielding the relations

$$\begin{aligned} 2p \cdot q &= \hat{s} + Q^2, \\ \hat{u} &= m_f^2 + m_{f'}^2 - Q^2 - \hat{s} - \hat{t}. \end{aligned} \tag{8}$$

As usually, we denote by s the (total) squared c.m.s. energy:

$$s := (P + l_e)^2 \approx 2P \cdot l_e \tag{9}$$

and by W the final hadronic mass:

$$W^2 := (P+q)^2. \tag{10}$$

In the following we assume the gluon to carry a fraction η of the proton momentum:

$$p = \eta P, \qquad \text{i.e. } p\cdot q = \eta P\cdot q, \ldots . \tag{11}$$

Then the squared c.m.s. energy s_G of the electron-gluon sub-system (4) equals

$$s_G := (p+l_e)^2 = 2p\cdot l_e = \eta s. \tag{12}$$

It is convenient to define the following dimensionless variables:

$$x := \frac{Q^2}{2P\cdot q},$$

$$x_G := \frac{Q^2}{2p\cdot q},$$

$$y := \frac{p\cdot q}{p\cdot l_e},$$

$$z := \frac{p\cdot p_f}{p\cdot q}. \tag{13}$$

We find the following relations

$$x = \eta x_G = \eta \frac{Q^2}{\hat{s}+Q^2},$$

$$y = \frac{\hat{s}+Q^2}{\eta s} = \frac{Q^2}{xs},$$

$$Q^2 = x_G y s_G = xys,$$

$$W^2 = \frac{1-x}{x}Q^2,$$

$$\hat{s} = (1-x_G)ys_G = ys(\eta - x) = Q^2\frac{\eta - x}{x} = Q^2\frac{1-x_G}{x_G},$$

$$\hat{t} = m_f^2 - zys_G. \tag{14}$$

3. Cross section formula

We define electromagnetic and weak couplings by the following interaction lagrangian densities:

$$\mathscr{L}_{\rm em} = -e\left[Q_{\rm e}\bar{\Psi}_{\rm e}\gamma^{\mu}\Psi_{\rm e} + Q_f\bar{\Psi}_f\gamma^{\mu}\Psi_f\right]A_{\mu},$$

$$\mathscr{L}_{\rm nc} = -\frac{e}{2\sin 2\theta_{\rm W}}\left[\bar{\Psi}_{\rm e}\gamma^{\mu}(v - a\gamma_5)\Psi_{\rm e} + \bar{\Psi}_f\gamma^{\mu}(v_f - a_f\gamma_5)\Psi_f\right]Z_{\mu},$$

$$\mathscr{L}_{\rm cc} = -\frac{e}{2\sqrt{2}\,\sin\theta_{\rm W}}\left[\bar{\Psi}_{\rm e}\gamma^{\mu}(1-\gamma_5)\Psi_{\nu} + \bar{\Psi}_f V_{ff'}\gamma^{\mu}(1-\gamma_5)\Psi_{f'}\right]W_{\mu}, \qquad (15)$$

where the Dirac fields $\Psi_{\rm e}, \Psi_{\nu}, \Psi_f$ ($\Psi_{f'}$) and the vector fields A_{μ}, Z_{μ} (W_{μ}) describe, respectively, the electron e^-, the electron-neutrino, the quark with flavour $f(f')$, the photon γ and the neutral intermediate boson Z^0 (W) of mass $m_{\rm Z}$ ($m_{\rm W}$); $Q_{\rm e}$ and Q_f give the electric charge of e^- and quark of flavour f in units of $e = \sqrt{4\pi\alpha}$, where α is the fine structure constant. $V_{ff'}$ is the Kobayashi-Maskawa quark mixing matrix and $\theta_{\rm W}$ is the Weinberg angle. The parameters v (v_f) and a (a_f) determine the strength of the vector and axial vector couplings of the Z^0 at the electron (quark) vertex. One has for:

(i) charged leptons

$$Q_e = -1, \qquad v = -1 + 4\sin^2\theta_{\rm W}, \qquad a = -1,$$

(ii) neutral leptons

$$Q_e = 0, \qquad v = +1, \qquad a = +1, \qquad (16)$$

(iii) u, c, t, ... quarks

$$Q_f = \tfrac{2}{3}, \qquad v_f = +1 - \tfrac{8}{3}\sin^2\theta_{\rm W}, \qquad a_f = +1,$$

(iv) d, s, b, ... quarks

$$Q_f = -\tfrac{1}{3}, \qquad v_f = -1 + \tfrac{4}{3}\sin^2\theta_{\rm W}, \qquad a_f = -1.$$

The masses of Z^0 and W are given by:

$$m_{\rm W}^2 = \frac{\pi\alpha}{G_{\rm F}\sin^2\theta_{\rm W}(1-\Delta r)\sqrt{2}},$$

$$m_{\rm Z}^2 = \frac{m_{\rm W}^2}{\cos^2\theta_{\rm W}}, \qquad (17)$$

where G_F is the Fermi weak coupling constant and Δr an electroweak radiative correction.

The cross section for producing a quark-antiquark pair of flavour f (ff' in the charged sector) is given by the formula*:

$$d\sigma_f^{\pm} = \frac{1}{4p\cdot l}\frac{1}{2}\frac{1}{2}\theta_l\, G(\eta,\hat{s})\, d\eta\, dPS^{(3)} \sum_{\text{spins}} |\mathcal{M}_f^{\pm}|^2 . \tag{18}$$

Here $G(\eta,\hat{s})$ is the gluon distribution (normalized to $\frac{1}{2}$), and gluon spin- and colour-average factors ($\frac{1}{2}$ and $\frac{1}{2}$) have been included. θ_l equals $\frac{1}{2}(1)$ for an incoming electron (neutrino). The momentum scale of the gluon denity has been chosen to correspond to the total invariant energy $\hat{s}$ of the produced heavy quark system. This scale $\hat{s}$ has also been used as argument of the running QCD coupling constant g_s:

$$\alpha_s(\hat{s}) = \frac{12\pi}{(33-2N_f)\ln(\hat{s}/\Lambda^2)} . \tag{19}$$

In sect. 7 we will further comment on this choice as well as on the choice of Λ and the number of flavours N_f.

In the appendix we will show that the most general cross section can be written as:

$$d\sigma_{ff'}^{\pm} = \frac{(2\pi)^3\alpha_s(\hat{s})\alpha^2 2\theta_l}{yQ^4} G(\eta,\hat{s})\, d\eta\, dPS^{(3)}\left\{ g_{11}^{ff';\pm}A_{11} + g_{12}^{ff';\pm}A_{12} + g_{44}^{ff';\pm}A_{44}\right\} . \tag{20}$$

The coefficients $g_{ij}^{ff';\pm}(Q^2)$ in (20) depend solely on Q^2 and on the electroweak coupling constants. In the neutral sector they contain all the information on γ-Z^0 interference and the Z^0-boson itself. Explicitly we have:

$$\begin{aligned}
g_{11}^{f;\pm} &= Q_f^2 + 2Q_f v_f \Re(\chi_Z)(-v \mp \rho a) + \left(v_f^2 + a_f^2\right)|\chi_Z|^2\left(v^2 + a^2 \pm 2va\rho\right),\\
g_{12}^{f;\pm} &= Q_f^2 + 2Q_f v_f \Re(\chi_Z)(-v \mp \rho a) + \left(v_f^2 - a_f^2\right)|\chi_Z|^2\left(v^2 + a^2 \pm 2va\rho\right),\\
g_{44}^{f;\pm} &= 2Q_f a_f \Re(\chi_Z)(\pm a + v\rho) + 2v_f a_f|\chi_Z|^2\left(\mp 2va - \rho(v^2+a^2)\right).
\end{aligned} \tag{21}$$

Here $\chi_Z(Q^2)$ is the ratio of the Z^0-propagator to the photon propagator times a coupling strength factor:

$$\chi_Z(Q^2) = \frac{1}{(2\sin 2\theta_W)^2}\frac{Q^2}{Q^2 + m_Z^2 - im_Z\Gamma_Z} \tag{22}$$

* "+" and "−" refer to positron and electron scattering, respectively.

and ρ is the degree of longitudinal polarization of the electron (positron) with $\rho = -1\ (+1)$ for a left- (right-) handed lepton.

In the charged current case the electroweak couplings are:

$$g_{11}^{ff';\pm} = 4|V_{ff'}|^2|\chi_W|^2(1 \pm \rho),$$

$$g_{12}^{ff';\pm} = 0,$$

$$g_{44}^{ff';\pm} = 4|V_{ff'}|^2|\chi_W|^2(\mp 1 - \rho). \tag{23}$$

Here $\chi_W(Q^2)$ is defined by:

$$\chi_W(Q^2) = \frac{1}{\left(2\sqrt{2}\sin\theta_W\right)^2}\frac{Q^2}{Q^2 + m_W^2 - im_W\Gamma_W}. \tag{24}$$

The quantities A_{11}, A_{12}, A_{44} in (20), finally, are given by ($i = 1,2$; see appendix):

$$A_{1i} \equiv \frac{y}{2s_G}L_1^{\mu\nu}H_{\mu\nu}^i = x_G y^2 G_1^{(i)}(x_G, z, y, s_G) + (1-y)G_2^{(i)}(x_G, z, y, s_G)$$

$$+ (2-y)\sqrt{1-y}\cos\Phi\, G_A^{(i)}(x_G, z, y, s_G)$$

$$+ 2x_G(1-y)\cos 2\Phi\, G_B^{(i)}(x_G, z, y, s_G),$$

$$A_{44} \equiv \frac{y}{2s_G}L_4^{\mu\nu}H_{\mu\nu}^4 = x_G y(2-y)G_3(x_G, z, y, s_G)$$

$$+ 2y\sqrt{1-y}\cos\Phi\, G_C(x_G, z, y, s_G). \tag{25}$$

The (partonic) structure functions $G_l^{(i)} \equiv G_l^{(i)}(x_g, z; y, s_G)$ are given explicitly in the appendix. Here we want to emphasize that the $G_l^{(i)}$ depend explicitly on the variable y. This differs from what is found in the massless quark case [14,15] where $G_l^{(i)}$ depend on z and x_G solely. Thus the decomposition of the total cross section in different y-dependent terms à la (25) does not exhibit the full y-structure in the massive case.

4. Phase space

In this section we present an explicit representation of the particle momenta and investigate the physical region boundaries. We find it convenient to work in the final-state-quark (or boson-gluon) c.m.s. defined by

$$\boldsymbol{p}_f + \boldsymbol{p}_{f'} = 0 = \boldsymbol{p} + \boldsymbol{q}, \tag{26}$$

where the gluon momentum $\boldsymbol{p}$ and thereby the proton momentum $\boldsymbol{P}$ points into the positive z-direction. We define Φ to be the angle between the lepton plane $(\boldsymbol{p}\times\boldsymbol{l}_e)$ and the hadron plane $(\boldsymbol{p}\times\boldsymbol{p}_f)$*:

$$\cos\Phi := \frac{(\boldsymbol{p}\times\boldsymbol{l}_e)\cdot(\boldsymbol{p}\times\boldsymbol{p}_f)}{|\boldsymbol{p}\times\boldsymbol{l}_e|\,|\boldsymbol{p}\times\boldsymbol{p}_f|}\,. \tag{27}$$

An explicit representation of the particle momenta is provided by:

$$\begin{aligned}
p &= (E_p, 0, 0, E_p)\,,\\
q &= (Q_0, 0, 0, -E_p)\,,\\
l_e &= E_{\ell}(1, \sin\beta, 0, \cos\beta)\,,\\
p_f &= (E_1, q_1\sin\theta\cos\Phi, q_1\sin\theta\sin\Phi, q_1\cos\theta)\,,\\
p_{f'} &= (E_2, -q_1\sin\theta\cos\Phi, -q_1\sin\theta\sin\Phi, -q_1\cos\theta)\,,
\end{aligned} \tag{28}$$

where

$$\begin{aligned}
E_p &= E(\hat{s}, 0, -Q^2)\,,\\
Q_0 &= E(\hat{s}, -Q^2, 0)\,,\\
E_l &= E(\hat{s}, 0, t_3)\,,\\
E_1 &= E(\hat{s}, m_f^2, m_{f'}^2)\,,\\
E_2 &= E(\hat{s}, m_{f'}^2, m_f^2)\,,\\
q_1 &= P(\hat{s}, m_f^2, m_{f'}^2)\,,\\
\cos\beta &= \frac{2E_pE_1 - s_G}{2E_pE_l}\,,\\
\cos\theta &= \frac{2E_pE_1 - m_f^2 + \hat{t}}{2E_pq_1}\,,
\end{aligned} \tag{29}$$

* The authors of [14] consider the hadronic c.m.s. $\boldsymbol{P}+\boldsymbol{q}=0$, where the protron momentum points in the negative z-direction. To coincide with their notation simply replace $\cos\Phi$ by $(-\cos\Phi)$ in our final results and leave terms proportional to 1 and $\cos 2\Phi$ unchanged.

and

$$t_3 = (p - l_e)^2 = -s_G + \hat{s} + Q^2,$$

$$E(x, y, z) = \frac{x + y - z}{2\sqrt{x}},$$

$$P(x, y, z) = \sqrt{\frac{x^2 + y^2 + z^2 - 2xy - 2xz - 2yz}{4x}}. \tag{30}$$

The 3-particle phase space is then given by

$$128\pi^3 \mathrm{dPS}^{(3)} = \frac{\mathrm{d}\hat{s}\,\mathrm{d}Q^2\,\mathrm{d}\hat{t}}{s_G(\hat{s} + Q^2)} \frac{\mathrm{d}\Phi}{2\pi} = s_G y\,\mathrm{d}y\,\mathrm{d}x_G\,\mathrm{d}z \frac{\mathrm{d}\Phi}{2\pi}. \tag{31}$$

Note that

$$\mathrm{d}z \frac{\mathrm{d}\Phi}{2\pi} = 8\pi\,\mathrm{dPS}^{(2)}, \tag{32}$$

where $\mathrm{dPS}^{(2)}$ is the two-particle phase space for the process (5): $p + q \to p_f + p_{f'}$.

In total there are 5 independent integration variables. Looking at the restraints provided by individual angles we can find the physical region boundaries. The integration region for the Φ-integration is simply $[0, 2\pi]$. The condition $-1 \leqslant \cos\theta(p, p_f) \leqslant +1$ yields the $\hat{t}$-integration bounds:

$$\hat{t}_{\min} := m_f^2 - \frac{\hat{s} + Q^2}{2\hat{s}}(\gamma^2 + \sqrt{\lambda}),$$

$$\hat{t}_{\max} := m_f^2 - \frac{\hat{s} + Q^2}{2\hat{s}}(\gamma^2 - \sqrt{\lambda}), \tag{33}$$

or equivalently:

$$z_{\max} := \frac{\gamma^2 + \sqrt{\lambda}}{2\hat{s}},$$

$$z_{\min} := \frac{\gamma^2 - \sqrt{\lambda}}{2\hat{s}}. \tag{34}$$

Here we have defined:

$$\gamma^2 := \hat{s} + m_f^2 - m_{f'}^2 = s_G y(1 - x_G) + m_f^2 - m_{f'}^2,$$

$$\lambda := (\hat{s} - m_f^2 - m_{f'}^2)^2 - 4m_f^2 m_{f'}^2$$

$$= (s_G y(1 - x_G) - m_f^2 - m_{f'}^2)^2 - 4m_f^2 m_{f'}^2. \tag{35}$$

Considering $(p_f + p_{f'})^2$ gives us

$$\hat{s} \geqslant \hat{s}_0 := (m_f + m_{f'})^2, \tag{36}$$

whereas baryon number conservation imposes the cut

$$W^2 := (P+q)^2 = m_p^2 + \frac{\hat{s}+Q^2}{\eta} - Q^2$$

$$\geqslant W_0^2 := (m_f + m_{f'} + m_p)^2. \tag{37}$$

Examination of the lower limit of Q^2 gives [16]:

$$Q^2 \geqslant m_e^2 \frac{y^2}{1-y} \equiv Q^2_{\min}. \tag{38}$$

However, in order to investigate the dependence of the cross section on the lower limit $Q^2_{\min}$ of Q^2 we will present numerical values for the total cross section for various values of $Q^2_{\min}$. The last constraint arising from

$$t_3 = (p-l)^2 \leqslant t_{3_{\max}} \equiv 0, \tag{39}$$

can be written as

$$\eta s - \hat{s} - Q^2 \geqslant 0. \tag{40}$$

Collecting these constraints we obtain for the physical region boundaries:

$$128\pi^3 \int \mathrm{d}\eta \, \mathrm{dPS}^{(3)} = \Theta\left(s + 2m_e^2 - 2\sqrt{m_e^2(s+m_e^2)} - W_1^2\right)$$

$$\times \int_{y_{\min}}^{y_{\max}} \mathrm{d}y \int_{Q^2_{\min}(y)}^{Q^2_{\max}(y)} \mathrm{d}Q^2 \int_{\eta_{\min}(y,Q^2)}^{1} \mathrm{d}\eta \int_{z_{\min}(y,Q^2,\eta)}^{z_{\max}(y,Q^2,\eta)} \mathrm{d}z \int_0^{2\pi} \frac{\mathrm{d}\Phi}{2\pi}, \tag{41}$$

where

$$\eta_{\min}(y,Q^2) := \frac{\hat{s}_0 + Q^2}{ys},$$

$$Q^2_{\max}(y) := ys - W_1^2,$$

$$y_{\max,\min} := \frac{s + W_1^2 \pm \sqrt{(s-W_1^2)^2 - 4m_e^2 W_1^2}}{2(s+m_e^2)},$$

$$W_1^2 := W_0^2 - m_p^2. \tag{42}$$

Using x instead of $Q^2 = xys$ as second integration variable we obtain the following limits:

$$x_{\min} = \frac{m_e^2}{s}\frac{y}{1-y},$$

$$x_{\max} = 1 - \frac{W_1^2}{ys}. \tag{43}$$

We finally mention that the transverse momentum of the quark (antiquark) with respect to the proton direction is defined by

$$p_T = \pm |\boldsymbol{p}_f^{(12)}| \sin\theta^{(12)}, \tag{44}$$

where (12) denotes the c.m.s. $\boldsymbol{p}_f + \boldsymbol{p}_{f'} = 0$ with $\boldsymbol{p}$ pointing into the positive z direction. We find

$$p_T^2 = \hat{s}z(1-z) + z\left(m_f^2 - m_{f'}^2\right) - m_f^2. \tag{45}$$

5. Total cross section

The total, five-fold differential cross section is now given by:

$$\begin{aligned} \mathrm{d}\sigma_{ff'}^{\pm} = \mathrm{d}y\,\mathrm{d}Q^2\,\mathrm{d}\eta\,\mathrm{d}z \frac{\mathrm{d}\Phi}{2\pi}\frac{\alpha_s(\hat{s})\alpha^2 2\theta_l}{16yQ^4} G(\eta,\hat{s}) \\ \times\Big[g_{11}^{ff';\pm}\big\{ x_G y^2 G_1^{(1)}(x_G,z;y,s_G) + (1-y)G_2^{(1)}(x_G,z;y,s_G) \\ + (2-y)\sqrt{1-y}\cos\Phi\, G_A^{(1)}(x_G,z;y,s_G) \\ + 2x_G(1-y)\cos 2\Phi\, G_B^{(1)}(x_G,z;y,s_G)\big\} \\ + g_{12}^{ff';\pm}\big\{ x_G y^2 G_1^{(2)}(x_G,z;y,s_G) + (1-y)G_2^{(2)}(x_G,z;y,s_G)\big\} \\ + g_{44}^{ff';\pm}\big\{ x_G y(2-y)G_3(x_G,z;y,s_G) \\ + 2y\sqrt{1-y}\cos\Phi\, G_C(x_G,z;y,s_G)\big\}\Big]. \end{aligned} \tag{46}$$

The integration regions are given in (41). This is the most general form of the cross section $\mathrm{d}\sigma^{\pm}$ for positron (electron) scattering on protons into heavy flavours. If the couplings $g_{ij}^{f;\pm}$ are given by (21) and we take $m_{f'} = m_f$ in the partonic structure functions $G_\ell^{(k)}$, then (46) gives the cross section for producing a heavy quark-antiquark pair of flavour f in the neutral sector including the γ-Z^0 interference. In the charged current sector we have to be aware of the assignment of the quark masses:

We arrive at the cross section for producing a heavy up-like quark of flavour f and a heavy down-like antiquark of flavour f' in e^+p-scattering by using $g_{ij}^{ff';+}$ as defined in (23) and taking m_f ($m_{f'}$) as the mass of the up- (down-) like quark in the partonic structure functions $G_\ell^{(k)}$. For the production of a heavy down-like quark and a heavy up-like antiquark in e^-p scattering we have to use $g_{ij}^{ff';-}$ and the opposite assignment of the masses. For example, in $e^+p \to t\bar{b}$ we need $m_f = m_t$, $m_{f'} = m_b$, whereas in $e^-p \to \bar{t}b$ we have to take $m_f = m_b$, $m_{f'} = m_t$. The parameter ρ in (21) and (23) accounts for a possible longitudinal polarization of the incoming lepton.

From (46) many interesting differential distributions can be calculated, such as the p_T distribution of the heavy quarks or the asymmetry in the angle Φ. Here, however, we restrict ourselves to the total integrated cross section. We find that two of the five integrations can be done analytically. These integrations will just eliminate the inner structure of the final state (see eq. (32)) and yield the contributions of the heavy flavours to the deep-inelastic (DIS) structure functions.

The Φ-integration is trivial, it just eliminates the Φ-dependent terms in (46). Besides the Φ-integration the z-integration can be done analytically. Let us define:

$$\int_{z_{\min}}^{z_{\max}} dz \int_0^{2\pi} \frac{d\Phi}{2\pi} G_j^{(i)} =: R_j^{(i)}(x_G; y, s_G). \tag{47}$$

Then we obtain:

$$\begin{aligned}
R_1^{(1)} &= -\frac{16\sqrt{\lambda}}{y s_G (1-x_G)}\left(4x_G^2 - 4x_G + 1\right) \\
&\quad + 8\Psi\left(2x_G^2 - 2x_G + 1 + 2m_-^4 - 4x_G m_-^2 + 2m_-^2\right) \\
&\quad + 8\tilde{\Psi}\left(2x_G^2 - 2x_G + 1 + 2m_-^4 + 4x_G m_-^2 - 2m_-^2\right), \\
R_1^{(2)} &= -\frac{64 m_0 \sqrt{\lambda}}{y s_G} + 32 m_0 (1 - x_G - m_+^2)(\Psi + \tilde{\Psi}), \\
R_2^{(1)} &= 2x_G R_1^{(1)} + \frac{64\sqrt{\lambda}}{y s_G}\left(2x_G^2 - x_G m_+^2 + m_-^4\right) \\
&\quad + 16\Psi\left\{-2x_G m_+^4 + 2m_+^2 m_-^4 + m_+^2\left(-6x_G^2 + 2x_G + 1\right)\right. \\
&\qquad \left. + 2m_-^4(3x_G - 1) + 4m_-^2 x_G (1 - 2x_G)\right\} + 16\tilde{\Psi}\{m_f \leftrightarrow m_{f'}\}, \\
R_2^{(2)} &= -32 m_0 (\Psi + \tilde{\Psi}), \\
R_3 &= \frac{32 m_-^2 \sqrt{\lambda}}{y s_G} + 8\Psi\left(-2x_G^2 + 2x_G - 1 + 4x_G m_-^2 + 2m_-^2 m_+^2 - 2m_-^2\right) \\
&\quad - 8\tilde{\Psi}\left(-2x_G^2 + 2x_G - 1 - 4x_G m_-^2 - 2m_-^2 m_+^2 + 2m_-^2\right).
\end{aligned} \tag{48}$$

Here we have defined:

$$\Psi = \ln \frac{\gamma^2 + \sqrt{\lambda}}{\gamma^2 - \sqrt{\lambda}},$$

$$\tilde{\Psi} = \Psi(m_f \leftrightarrow m_{f'}). \tag{49}$$

γ and λ have already been defined in (35), and $m_{\pm}^2$, m_0 are defined in (75).

Note that $R_1^{(i)}$ and $R_2^{(i)}$ $(i = 1,2)$ are symmetric under the exchange of m_f and $m_{f'}$, whereas R_3 is antisymmetric under this exchange. Thus R_3 is zero in the neutral case.

The Φ- and z-integrated cross section can now be written as:

$$\begin{aligned}
\sigma_{ff'}^{\pm} = \int_{y_{\min}}^{y_{\max}} \mathrm{d}y \int_{Q^2_{\min}}^{Q^2_{\max}} \mathrm{d}Q^2 \int_{\eta_{\min}}^{1} \mathrm{d}\eta \, \frac{\alpha_s(\hat{s})\alpha^2 2\theta_l}{16 y Q^4} G(\eta, \hat{s}) \\
\times \Big[g_{11}^{ff';\pm} \{ x_G y^2 R_1^{(1)}(x_G; y, s_G) + (1-y) R_2^{(1)}(x_G; y, s_G) \} \\
+ g_{12}^{ff';\pm} \{ x_G y^2 R_1^{(2)}(x_G; y, s_G) + (1-y) R_2^{(2)}(x_G; y, s_G) \} \\
+ g_{44}^{ff';\pm} x_G y(2-y) R_3(x_G; y, s_G) \Big] \\
\times \Theta\Big(s + 2m_e^2 - 2\sqrt{m_e^2 (s + m_e^2)} - W_1^2 \Big).
\end{aligned} \tag{50}$$

We finally want to express the usual DIS structure functions F_i $(i = 1,2,3)$ by the partonic structure functions $R_i^{(j)}$. We start from the usual definitions for F_i:

$$\begin{aligned}
\mathrm{d}\sigma_f^{\pm} = \mathrm{d}x \, \mathrm{d}y \frac{4\pi\alpha^2}{Q^2 x y} \Theta(y - y_{\min}) \Theta(y_{\max} - y) \Theta(x - x_{\min}(y)) \Theta(x_{\max}(y) - x) \\
\times \Theta\Big(s + 2m_e^2 - 2\sqrt{m_e^2 (s + m_e^2)} - W_1^2 \Big) \\
\times \Big[g_{11}^{f;\pm} \{ x y^2 F_1(x, Q^2) + (1-y) F_2(x, Q^2) \} + g_{44}^{f;\pm} x y (2-y) F_3(x, Q^2) \Big].
\end{aligned} \tag{51}$$

For the charged current sector it is sometimes more convenient to write (51) in the following way:

$$\begin{aligned}
\mathrm{d}\sigma_{ff'}^{\pm} = \mathrm{d}x \, \mathrm{d}y \frac{G_F^2 s}{2\pi} \frac{|V_{ff'}|^2 (1 - \Delta r)^2}{(1 + Q^2/m_W^2)^2} \Theta(y - y_{\min}) \Theta(y_{\max} - y) \Theta(x - x_{\min}(y)) \\
\times \Theta(x_{\max}(y) - x) \Theta\Big(s + 2m_e^2 - 2\sqrt{m_e^2 (s + m_e^2)} - W_1^2 \Big) \\
\times \Big[(1 \pm \rho) \{ x y^2 F_1(x, Q^2) + (1-y) F_2(x, Q^2) \} \\
- (\pm 1 + \rho) x y (2-y) F_3(x, Q^2) \Big].
\end{aligned} \tag{52}$$

We then find the following relations ($a = x + \hat{s}_0/(ys)$):

$$F_1(x,Q^2) = \frac{\alpha_s(\hat{s})}{2\pi}\frac{2\theta_l}{32}\int_a^1 \frac{d\eta}{\eta} G(\eta,\hat{s})\left[R_1^{(1)}(x_G,y,s_G) + \frac{g_{12}^{f_i\pm}}{g_{11}^{f_i\pm}} R_1^{(2)}(x_G,y,s_G)\right],$$

$$F_2(x,Q^2) = \frac{\alpha_s(\hat{s})}{2\pi}\frac{2\theta_l}{32}\int_a^1 d\eta\, G(\eta,\hat{s})\left[R_2^{(1)}(x_G,y,s_G) + \frac{g_{12}^{f_i\pm}}{g_{11}^{f_i\pm}} R_2^{(2)}(x_G,y,s_G)\right],$$

$$F_3(x,Q^2) = \frac{\alpha_s(\hat{s})}{2\pi}\frac{2\theta_l}{32}\int_a^1 \frac{d\eta}{\eta} G(\eta,\hat{s}) R_3(x_G,y,s_G). \tag{53}$$

However, several comments should be added. Firstly, in the NC sector the cross section develops a new dependence on the standard electroweak couplings via the $g_{12}^{f_i\pm}/g_{11}^{f_i\pm}$ terms in (53) ($g_{12}^{CC} = 0$). Secondly, we emphasize that the hadronic structure functions F_i are explicitly y-dependent for massive quarks: $F_i = F_i(y)$. This differs from the $O(\alpha_s)$ result of massless QCD where the partonic structure functions $R_l^{(i)}$ depend solely on x_G [14]. There the cross section becomes Q^2-dependent only via the use of a Q^2-dependent gluon density (and/or a Q^2-dependent α_s). The third comment concerns the use of (51) as a starting function to generate the variables (x, y) via a Monte Carlo event generator program. Contrary to the massless case one cannot avoid to perform an integration, see (53). Finally we mention that the e^-p- and e^+p-cross sections are the same as long as the leptons are unpolarized ($\rho = 0$). The "$\pm$" sign in (52) in front of F_3 cancels against the antisymmetry of F_3 in $m_f \leftrightarrow m_{f'}$.

6. Weizsäcker-Williams approximation

The Weizsäcker-Williams approximation (WWA) provides a convenient framework to derive simple approximate forms of the previous formulae. These may be useful for several reasons. On the one hand the above expressions are unnecessarily complicated for many purposes. On the other hand, approximate formulae have existed for quite a long time [9]. These were used as guess for the total rates expected for heavy quarks at HERA. By comparison with the exact calculation of the previous sections we shall be able to specify the accuracy limits for these approximations.

For an inelastic process like (1) the double pole at $Q^2 = 0$ in the rate arising from the photon propagator is reduced to a simple pole by a corresponding zero in the numerator. The remaining singularity leads to a logarithmic term in the cross section. When the logarithmic term for photon exchange is large enough, the cross section is well approximated by only taking this term correctly into account. This is precisely what is done in the WWA where the cross section (1) is described by a

convolution of the probability for emitting a photon from the lepton vertex with the corresponding real photon cross section at the hadron vertex.

For process (1) the WWA gives:

$$\sigma_f^{\pm}(s) = \int_{y_{\min}}^{1} \mathrm{d}y P_\gamma(y) \int_{\eta_{\min}}^{1} \mathrm{d}\eta G(\eta, M^2) \hat{\sigma}_f(\hat{s}), \tag{54}$$

where P_γ is related to the probability of finding a photon in the positron (electron):

$$P_\gamma = \frac{\alpha}{2\pi} \frac{1+(1-y)^2}{y} \ln \frac{Q_2^2}{Q_1^2}. \tag{55}$$

$\hat{\sigma}_f(\hat{s})$ is the cross section for production of the heavy quark-antiquark pair by a real photon of energy $\frac{1}{2}\sqrt{\hat{s}} = \frac{1}{2}\sqrt{y\eta s}$ (see eq. (14) with $Q^2 = 0 = x = x_G$).

Note that $\sigma_f^{\pm}$ depends on Q_1^2 which appears in (55) for P_γ. Also note that, as it is the case for all leading approximations, there is some ambiguity on the choice of Q_2^2, which also appears in (55) for P_γ. In the next section we shall discuss the dependences of the cross section on Q_1^2 and Q_2^2. As in the full Q^2-formula there still is another ambiguity. Whereas it might be reasonable to take Q as the mass scale M for the gluon density $G(\eta, M^2)$ and for the strong coupling constant $\alpha_s(M^2)$ in the full Q^2 formula (at least for high Q^2), this choice clearly cannot be maintained for low Q^2. Thus we will take $M^2 = \hat{s}$ as in the full Q^2 case.

We now shortly describe the calculation of $\hat{\sigma}_f$. Two possibilities are open. On the one hand we can start from the real process γ + gluon $\rightarrow$ q + $\bar{\text{q}}$. Or we can take the $Q^2 \rightarrow 0$ limit in the previous exact formulae. As a consistency check we will pursue both methods. Let us start on the first way.

The real photon process γ + gluon $\rightarrow$ q$\bar{\text{q}}$ is given by:

$$\frac{\mathrm{d}\hat{\sigma}_f}{\mathrm{d}\hat{t}} = \frac{\pi Q_f^2 \alpha \alpha_s}{\hat{s}^2} \left(\frac{v_1}{v_2} + \frac{v_2}{v_1} + \frac{4m_f^2 \hat{s}}{v_1 v_2} - \frac{4m_f^4 \hat{s}^2}{v_1^2 v_2^2} \right), \tag{56}$$

where $v_1 = m_f^2 - \hat{t}$, $v_2 = m_f^2 - \hat{u}$ and m_f is the heavy quark mass. Integration over $\hat{t}$ from $\hat{t}_{\min}$ to $\hat{t}_{\max}$ (see eq. (33)) yields:

$$\hat{\sigma}_f = \frac{\pi Q_f^2 \alpha \alpha_s}{y\eta s} \{ \Psi(2 + 2w - w^2) - 2\chi(1+w) \}. \tag{57}$$

Here $w = 4m_f^2/\hat{s} = 4m_f^2/(y\eta s)$, $\chi = \sqrt{1-w}$ and $\Psi = \ln((1+\chi)/(1-\chi)) = 2\ln(1+\chi)/\sqrt{w}$. Inserting (57) in (54) gives the ep cross section in the WWA.

The same result is arrived at by considering the $Q^2 \rightarrow 0$ limit (or equivalently $x_G \rightarrow 0$ limit) in the formulae of the last section. First note that in the pure

electromagnetic case:

$$g_{11}^{f_i\pm} = g_{12}^{f_i\pm} = Q_f^2; \qquad g_{44}^{f_i\pm} = 0. \tag{58}$$

Thus ($i = 1,2$):

$$L_i \equiv g_{11}^{f_i\pm} R_i^{(1)} + g_{12}^{f_i\pm} R_i^{(2)} = Q_f^2\left(R_i^{(1)} + R_i^{(2)}\right),$$

$$L_3 \equiv g_{44}^{f_i\pm} R_3 = 0. \tag{59}$$

Taking now the $Q^2 = 0$ limit we find:

$$L_1 = L_2 = 8Q_f^2\left\{\Psi(2 + 2w - w^2) - 2\chi(1 + w)\right\}. \tag{60}$$

Finally we obtain:

$$\begin{aligned}\frac{\alpha_s(\hat{s})\alpha^2 2\theta_l}{16yQ^4}\Big[& g_{11}^{f_i\pm}\left\{x_G y^2 R_1^{(1)}(x_G; y, s_G) + (1-y)R_2^{(1)}(x_G; y, s_G)\right\} \\ & + g_{12}^{f_i\pm}\left\{x_G y^2 R_1^{(2)}(x_G; y, s_G) + (1-y)R_2^{(2)}(x_G; y, s_G)\right\} \\ & + g_{44}^{f_i\pm} x_G y(2-y) R_3(x_G; y, s_G)\Big] \\ = \frac{1}{Q^2}\frac{\alpha}{2\pi}\frac{y^2 + 2(1-y)}{y}\hat{\sigma}, & \end{aligned} \tag{61}$$

which shows that both methods coincide.

7. Numerical results

As an application of the derived formulae for heavy flavour production we present in this section results for the total rates of top production at HERA and discuss their uncertainties. We restrict ourselves to unpolarized electron scattering and take $\sin^2\Theta_W = 0.226$, $\alpha = \frac{1}{137}$, $\Delta r = 0.0696$, $\sqrt{s} = 314$ GeV, $V_{tb} = 1$, $V_{td} = V_{ts} = 0$ and $m_b = 5$ GeV.

The uncertainty of the integrated cross section is now determined by essentially two* facts: On the one hand we are somewhat free in the choice of the mass scale for the gluon density and the mass scale for the strong coupling constant α_s. On the other hand we can use various parametrizations of the gluon density. However, in order to be consistent with the low energy data from which the parametrizations of the gluon density were extracted we choose Λ and the number of flavours N_f in the

* Using a running coupling constant $\alpha(Q^2)$ instead of $\alpha(0)$ will change the result by at most 12%.

TABLE 1
Top production rates at HERA for $\int L\,dt = 100\ \text{pb}^{-1}$ and $m_b = 5$ GeV

	$\bar{t}b$-rate	$t\bar{t}$-rate				
m_t	CC	NC	γ	Z	γ-Z	total rate top
30	53	974	973	1.2	0.36	2000
40	33	188	187	0.42	0.09	408
50	21	41	41	0.14	0.02	102
60	13	9.2	9.2	0.04	0.006	31
70	8.1	2.0	2.0	0.01	0.001	12
80	5.0	0.44	0.44	0.003	3E − 4	5.9
90	3.0	0.09	0.09	5E − 4	6E − 5	3.2
100	1.8	0.01	0.01	1E − 4	1E − 5	1.8

formula (19) for α_s according to the values used in the respective parametrization. Furthermore, we find it plausible to use the same mass scale M for the gluon density and for α_s.

Let us first present the total cross section for top production at HERA using a definite gluon parametrization [6] and a fixed choice of the above mentioned mass scale: $M^2 = \hat{s}$. In table 1 we give the number of top events for various top quark masses assuming an integrated luminosity of 100 pb^{-1}. The first two columns, denoted by "CC" and "NC", give the total number of $\bar{t}b$ and $t\bar{t}$ events, respectively. In the next three columns of table 1 we show the individual contributions to the $t\bar{t}$-rates coming from γ-exchange, Z-exchange and γ-Z interference. The last column of table 1 denoted by "total rate top" gives the total number of expected top events (i.e. t plus $\bar{t}$ events), again for $\int L\,dt = 100\ \text{pb}^{-1}$.

A graphical representation of table 1 can be found in fig. 1. Here the upper full line represents the total number of top events, whereas the lower lying full line, the dotted line, the dashed line and the dashed-dotted line denote the contributions coming from γ-exchange, Z-exchange, γ-Z interference and W-exchange, respectively.

We find that for a top mass of 50 GeV (i.e. just beyond the reach of SLC and LEP I) we expect ≈ 102 top events ($\int L\,dt = 100\ \text{pb}^{-1}$) and even for a top mass of 100 GeV still ≈ 2 top events. Thus the top quark can be searched for up to masses of ≈ 100 GeV. It is also remarkable [11] that for a top mass above ≈ 55 GeV the cross section is dominated by W-exchange. We can also see that both the Z-exchange and the pure γ-Z interference contributions are negligible for the total rate of top production. For comparison we give the number of b events ($m_b = 5$ GeV) to be expected at HERA in table 2. Here we assume a top mass of 50 GeV. All other parameters have the same values as for table 1. We find that the total number of b events is clearly dominated by γ-exchange and is fairly large.

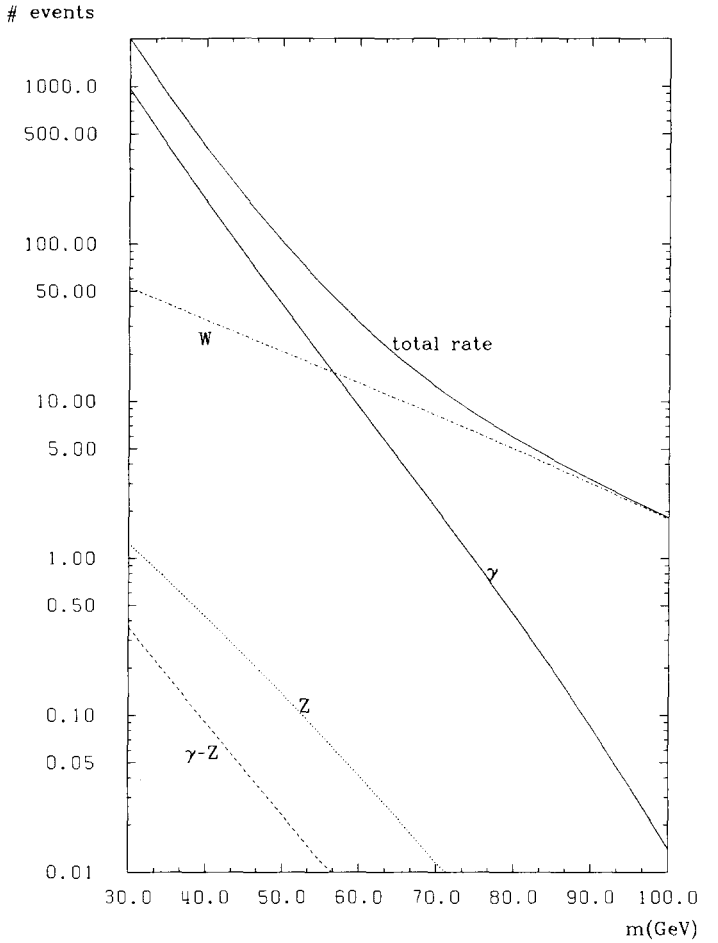

Fig. 1. Total top production rate. Number of top events versus top quark mass m for an integrated luminosity of $\int L\,dt = 100\ \text{pb}^{-1}$. The upper full line represents the total number of top events, whereas the lower lying full line, the dotted line, the dashed line and the dashed-dotted line denote the contributions coming from γ-exchange, Z-exchange, γ-Z-interference and W exchange, respectively. The gluon density G parametrization is from [6] and the mass scale M for G and α_s is $M^2 = \hat{s}$. All other parameters are given in the main text.

TABLE 2
Bottom production rates at HERA for $\int L\,dt = 100\ \text{pb}^{-1}$ and $m_t = 50$ GeV

m_b	$\bar{t}b$-rate	$b\bar{b}$-rate				total rate
	CC	NC	γ	Z	γ-Z	bottom
5	21	3.3E5	3.3E5	23	25	6.6E5

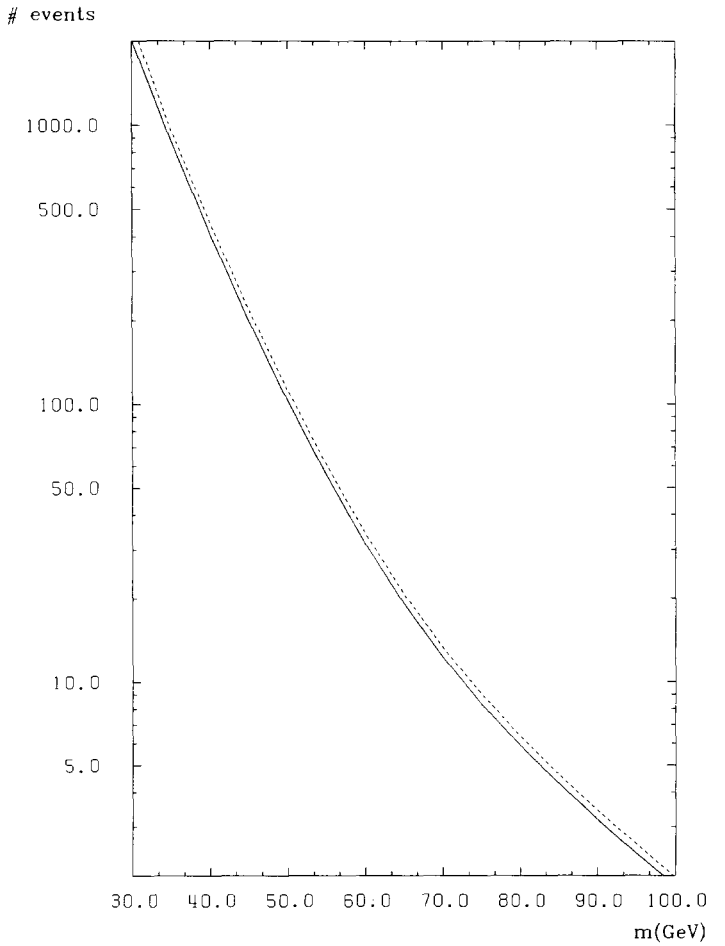

Fig. 2. Mass scale dependence of the cross section. Number of top events versus top quark mass m for an integrated luminosity of $\int L\,dt = 100\ \text{pb}^{-1}$. The two lines result from different mass scales M used for α_s and for the gluon density of [6] ($M^2 = \hat{s}$: full line; $M^2 = (m_t + m_b)^2$: dashed line). All other parameters are given in the main text.

Next we investigate the influence of the choice of the mass scale M on the total rates. We have checked that the changes in the cross sections are rather small as long as one chooses a scale like $\hat{s}$, $\hat{t}$ or $\hat{u}$. To give a feeling of the uncertainty due to different values for M we plot the total number of top events as a function of the top mass for two different choices of the mass scale M in fig. 2. (Again $\int L\,dt = 100\ \text{pb}^{-1}$ and the gluon density parametrization is from [6]). The full line in fig. 2 results from a calculation with $M^2 = \hat{s}$ whereas the dashed line is obtained using $M^2 = (m_t + m_b)^2$. Fig. 2 demonstrates that the uncertainty in the total rate is less than 10% over the whole mass range.

We now discuss the second uncertainty in the cross section which arises from the use of various parametrizations of the gluon density. We already mentioned that we always choose Λ and the number of flavours N_f according to the values used in the respective parametrization of the gluon density. In fig. 3 we plot the total rate of top production versus the top mass using five different parametrizations of the gluon density. Here we use $M^2 = \hat{s}$ and assume again $\int L\,dt = 100\ \text{pb}^{-1}$. The parametrizations set 1 and 2 of [18] are represented by the lower lying full and the lower lying

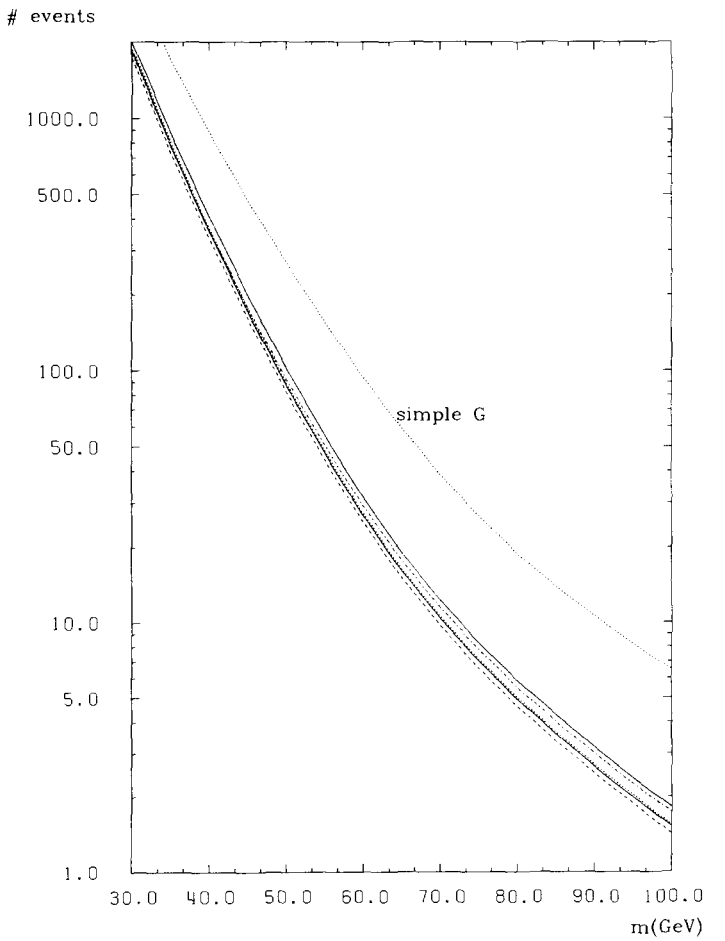

Fig. 3. Dependence on the parametrizations of the gluon density. Number of top events versus top quark mass m for an integrated luminosity of $\int L\,dt = 100\ \text{pb}^{-1}$. The six lines result from different parametrizations of the gluon density (set 1 of [18]: lower lying full line; set 2 of [18]: lower lying dotted line; set 1 of [17]: dashed line; set 2 of [17]: dashed-dotted line; [6]: upper lying full line). The upper lying dotted curve has been calculated using a scale independent gluon density $xG(x) = 3(1-x)^5$ and with $N_f = 5$, $\Lambda = 0.2$ GeV. The mass scale M is $M^2 = \hat{s}$. All other parameters are given in the main text.

dotted line, the parametrizations set 1 and 2 of [17] by the dashed and the dashed-dotted line, and the parametrization of [6] is represented by the upper lying full line, respectively. In fig. 3 we also give the result using the scale independent gluon density $xG(x) = 3(1-x)^5$ with $N_f = 5$ and $\Lambda = 0.2$ GeV. It corresponds to the upper lying dotted curve. We find that the uncertainty due to different parametrizations of the gluon density is $\leqslant 25\%$ over most of the mass range and tends to increase for increasing top mass. However, the scale independent gluon density overestimates the rate of top production by a factor of 2–5.

For experimental purposes it might be necessary to impose a lower cutoff in Q^2. It is therefore interesting to check how much one will lose in the total rate of top production. Since the photon exchange cross section is dominated by the low Q^2 region we expect the corresponding rate to depend strongly on the lower limit of Q^2. This should also be true for the total rate of $t\bar{t}$ production since the total NC rate is dominated by photon exchange.

The dependence of the top production rates on a lower cutoff Q_l^2 in Q^2, i.e.

$$\sigma = \int_{Q^2_{\min}}^{Q^2_{\max}} \mathrm{d}Q^2 \frac{\mathrm{d}\sigma}{\mathrm{d}Q^2} \Theta\left(Q^2 - Q_l^2\right) \text{ versus } Q_l^2$$

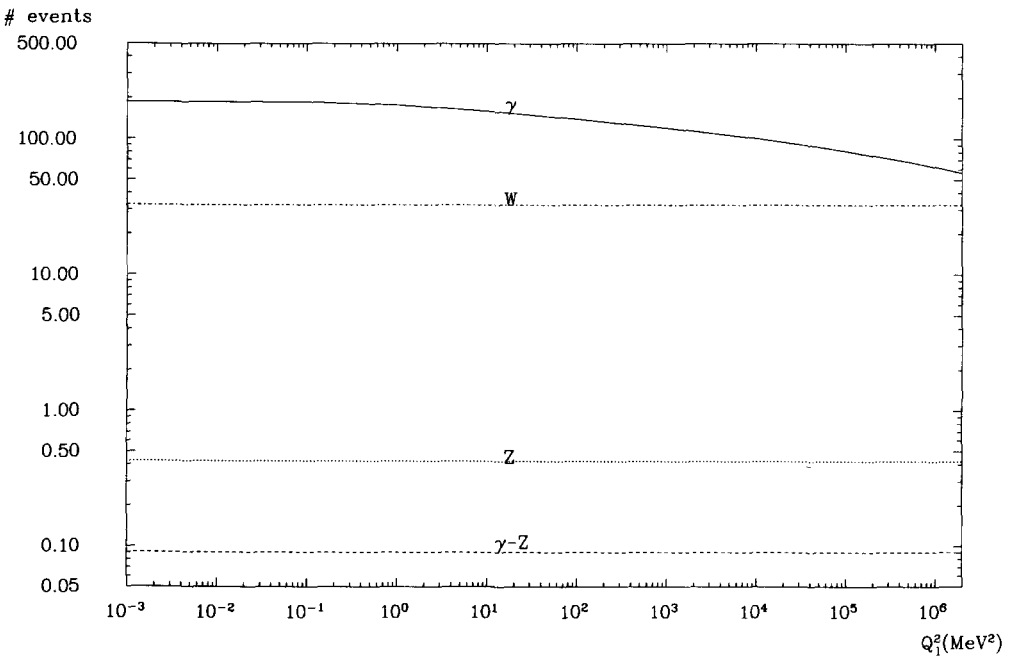

Fig. 4. Influence of a lower cutoff in Q^2. Individual contributions (number of events for $\int L\,\mathrm{d}t = 100$ pb^{-1}) to the top production cross section as a function of the lower cutoff Q_l^2 in Q^2: $\sigma = \int_{Q^2_{\min}}^{Q^2_{\max}} \mathrm{d}Q^2\,(\mathrm{d}\sigma/\mathrm{d}Q^2)\Theta(Q^2 - Q_l^2)$ versus Q_l^2. The four lines represent the contributions from γ-exchange: full line; Z-exchange: dotted line; γ-Z interference: dashed line; W-exchange: dashed-dotted line. The gluon density parametrization is from [6], $M^2 = \hat{s}$ and the top quark mass was taken to be $m = 40$ GeV. All other parameters are given in the main text.

can be seen in fig. 4 for a top quark of 40 GeV. Here we give the number of top events versus Q_l^2 where we take the gluon density of [6], $M^2 = \hat{s}$ and $\int L\,dt = 100$ pb^{-1}. The contributions from γ-exchange, Z-exchange, γ-Z interference and W-exchange are represented by the full, dotted, dashed and dashed-dotted line, respectively.

We recognize the described Q_l^2-behaviour of the photon exchange contribution. In fact, increasing the lower limit Q_l^2 from the kinematical bound $\approx m_e^2(\hat{s}_0/s)^2$ up to 2 GeV^2 decreases the photonic rate by a factor of three. We also see that the contributions from Z-exchange and γ-Z interference are more or less unchanged but negligible. We thus conclude that for a top quark mass up to 50 GeV the total top production rate will be diminished by a factor of three when imposing a Q^2-cut of 2 GeV^2.

The situation, however, gets reversed for a top quark of mass greater than ≈ 55 GeV because then the total rate of top production is dominated by W-exchange. From fig. 4 we note that the rate of the W-exchange contribution is stable against a Q^2-cut. We thus conclude that the total rate of top production will be almost

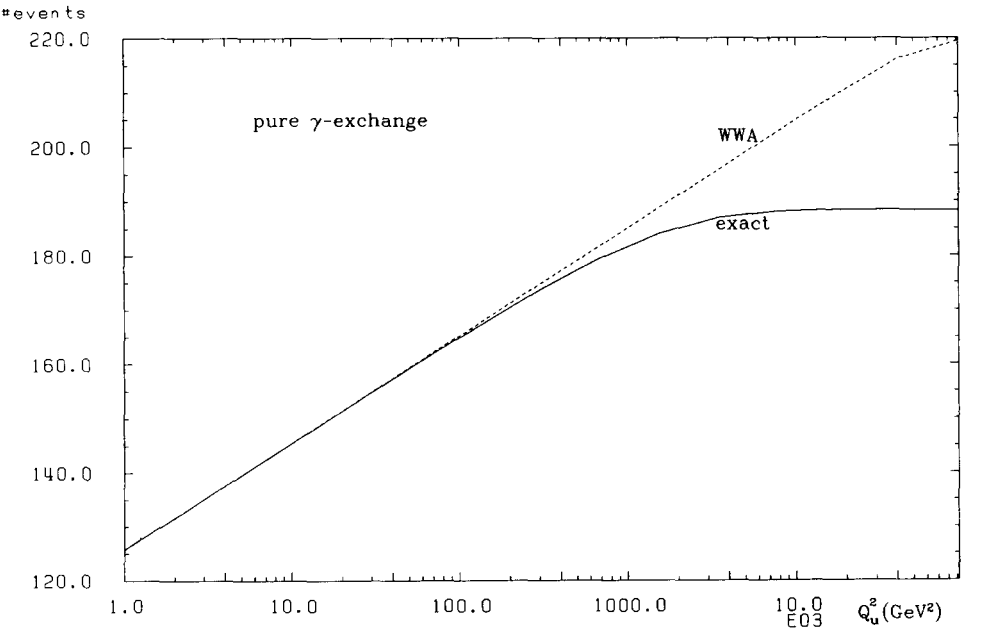

Fig. 5. Q^2_{cut} dependence of the WWA. Number of $t\bar{t}$ events for pure γ-exchange ($\int L\,dt = 100$ pb^{-1}) as a function of an upper cutoff Q_u^2 in Q^2: $\sigma = \int_{Q^2_{min}}^{Q_u^2} dQ^2 (d\sigma/dQ^2)\Theta(Q_u^2 - Q^2)$ versus Q_u^2. The full (dashed) line results from the full Q^2 (WWA) formula where we used the upper bound and lower bound of Q^2 in (55) for the WWA as given by the exact values in (38) and (42). The gluon density parametrization is from [6] and the top quark mass was taken to be $m = 40$ GeV. All other parameters are given in the main text.

unchanged by imposing a lower cut in Q^2 for $m_t \geqslant 55$ GeV. In particular, we still expect ≈ 2 top events for a 100 GeV top quark (if, again, $\int L\,dt = 100\ \text{pb}^{-1}$).

Let us now investigate the range of validity of the WWA. Clearly, since W-exchange becomes more and more important as the heavy quark mass increases we expect the WWA to be valid only for quarks with relatively low masses. However, in regions where the cross section is dominated by photon exchange ($m \leqslant 40$ GeV) the WWA is certainly applicable.

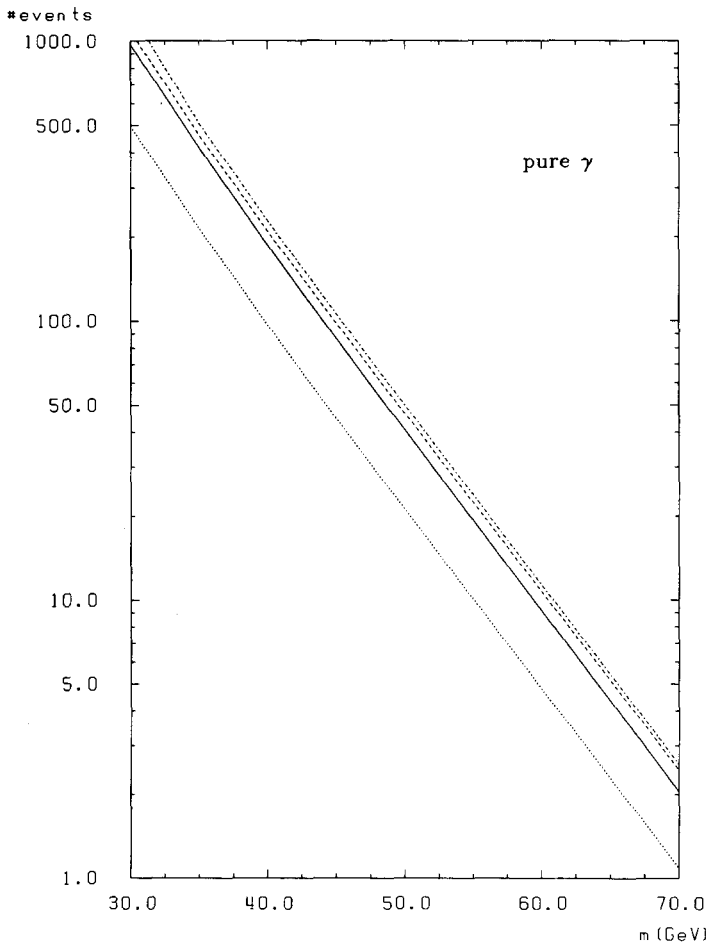

Fig. 6. Accuracy limits of the WWA. Number of $t\bar{t}$ events for pure γ-exchange ($\int L\,dt = 100\ \text{pb}^{-1}$) versus top quark mass m. The full line results from the full Q^2 formula. The dotted line, the dashed line and the dashed-dotted line result from the WWA using as lower and upper bound on Q^2: (m_e^2, m_π^2), $(m_e^2, \hat{s})$, $(m_e^2, s - 4m^2)$, respectively. The gluon density parametrization is from [6]. All other parameters are given in the main text.

We already mentioned that the WWA does not only depend on the lower cutoff Q_1^2 of Q^2 but also on the upper limit Q_2^2 via the $\ln(Q_2^2/Q_1^2)$ term in (55). We note that we would overestimate the cross section if in (55) we chose a scale for Q_2^2 of the order of the total c.m.s. energy squared s (this is the preferred choice in e^+e^- collisions). This overestimation still remains if the cuts Q_1^2 and Q_2^2 are given by the values of the exact Q^2-formula, i.e. if $Q_1^2 = Q_{\min}^2$ and $Q_2^2 = Q_{\max}^2$ where $Q_{\max,\min}^2$ are given in (38), (42). The reason is that the logarithmic increase of the WWA is valid only for moderate values of Q_2^2. The deviation of the WWA from the exact formula for high Q^2 is demonstrated in fig. 5 where we plot the number of $t\bar{t}$ events ($m_t = 40$ GeV) coming from pure γ-exchange against an upper limit Q_u^2 of Q^2:

$$\sigma = \int_{Q_{\min}^2}^{Q_{\max}^2} dQ^2 \frac{d\sigma}{dQ^2} \Theta(Q_u^2 - Q^2) \text{ versus } Q_u^2.$$

The full (dashed) line results from the full Q^2 (WWA) formula. Here we have chosen the above mentioned cuts $Q_1^2 = Q_{\min}^2$ and $Q_2^2 = Q_{\max}^2$ for the WWA and used the gluon density parametrization of [6]. The decline of the WWA curve at the upper edge of Q_u^2 stems from the fact that the effective upper limit $Q_{2,\text{eff}}^2$ in (55) for the WWA formula is given by $Q_{2,\text{eff}}^2 = \min(Q_2^2, Q_u^2)$. In total we observe that the deviation between the exact formulation and the WWA is less than 7%.

Finally we want to determine the accuracy limits of the WWA over a wide range of the top mass. Note, however, that this investigation only makes sense if we restrict ourselves to $t\bar{t}$ production since for $m_t \geq 55$ GeV the $\bar{t}b$ production will dominate. To this end we plot in fig. 6 the number of $t\bar{t}$ events resulting from pure γ-exchange versus the heavy quark mass. The full line results from the exact formula whereas the dotted line, the dashed line and the dashed dotted line stem from the WWA using as lower and upper bound on Q^2: $(Q_1^2, Q_2^2) = (m_e^2, m_\pi^2)$, $(m_e^2, \hat{s})$, $(m_e^2, s - 4m_t^2)$, respectively. The gluon density parametrization is from [6] and $\int L\, dt = 100$ pb^{-1}. We find that the WWA curves are in good shape with the full Q^2-formula. The discrepancy is less than 20% except for the case where $(Q_1^2, Q_2^2) = (m_e^2, m_\pi^2)$ which slightly underestimates the $t\bar{t}$-rate.

I would like to thank my collegues in the working group on "Heavy Quark Physics at HERA" for many stimulating discussions. Especially the support of A. Ali is gratefully acknowledged. I warmly thank G. Ingelman, J.G. Körner, R. Rückl and U.-J. Wiese for frequent discussions. I thank A.S. Kronfeld for a careful reading of the manuscript.

Appendix

In this section we exhibit the angular correlations between the initial and final state and the hadronic QCD effects. We recast the final expression for the total

differential cross section in a form similar to the quark-parton model (QPM) formula. However, since the massive case possesses a richer electroweak and kinematic structure than the massless case, our discussions will be quite lengthy.

It is convenient to expand the squared matrix element for process (4) in the following way:

$$\sum_{\text{spins}} |\mathcal{M}^{\pm}_{ff'}|^2 = g_s^2 \frac{e^4}{Q^4} \sum_{i,j=1}^{4} g_{ij}^{ff';\pm}(Q^2) L_i^{\mu\nu} H_{\mu\nu}^j . \tag{62}$$

The expansion is a linear superposition of the various parity conserving (p.c.) and parity violating (p.v.) terms in the hadron tensors $H_{\mu\nu}^{JJ'}$ and lepton tensors $L_{\mu\nu}^{JJ'}$: We define four hermitian hadron tensors $H_{\mu\nu}^r$ $(r = 1, \ldots, 4)$ by:

$$\begin{aligned}
H_{\mu\nu}^1 &= \tfrac{1}{2}\left(H_{\mu\nu}^{VV} + H_{\mu\nu}^{AA}\right) = H_{\mu\nu}^{RR} + H_{\mu\nu}^{LL}, \\
H_{\mu\nu}^2 &= \tfrac{1}{2}\left(H_{\mu\nu}^{VV} - H_{\mu\nu}^{AA}\right) = H_{\mu\nu}^{LR} + H_{\mu\nu}^{RL}, \\
H_{\mu\nu}^3 &= \tfrac{1}{2} i\left(H_{\mu\nu}^{VA} - H_{\mu\nu}^{AV}\right) = i\left(H_{\mu\nu}^{LR} - H_{\mu\nu}^{RL}\right), \\
H_{\mu\nu}^4 &= \tfrac{1}{2}\left(H_{\mu\nu}^{VA} + H_{\mu\nu}^{AV}\right) = H_{\mu\nu}^{RR} - H_{\mu\nu}^{LL},
\end{aligned} \tag{63}$$

and similarly four lepton tensors $L_{\mu\nu}^j$. The superscripts V and A denote the contributions of the vector $(V_\mu = \langle f|J_\mu^V(0)|0\rangle)$ and axial-vector $(A_\mu = \langle f|J_\mu^A(0)|0\rangle)$ currents according to $H_{\mu\nu}^{JJ'} = \langle J_\mu J_\nu'^* \rangle$, $(J, J' = V, A)$, where $\langle \cdots \rangle$ means sum over the (final state) polarizations. The superscript L and R, on the other hand, refer to the contributions of the left-handed $(2L_\mu = V_\mu - A_\mu)$ and right-handed $(2R_\mu = V_\mu + A_\mu)$ currents used especially in neutrino reactions. Similar definitions apply to the lepton tensors $L_{\mu\nu}^j$. The (finally surviving) electroweak coupling coefficients $g_{ij}^{ff';\pm}(Q^2)$ appearing in (62) are given in the main text.

Since we neglect the lepton masses the lepton tensors are simply given by

$$\begin{aligned}
L_{\mu\nu}^1 &= 4\left(2l_{e\mu}l_{e\nu} - q_\mu l_{e\nu} - l_{e\mu}q_\nu + g_{\mu\nu} l_e \cdot q\right), \\
L_{\mu\nu}^2 &= 0, \\
L_{\mu\nu}^3 &= 0, \\
L_{\mu\nu}^4 &= -4i\varepsilon_{\mu\nu\rho\sigma} l_e^\rho q^\sigma .
\end{aligned} \tag{64}$$

The hadron tensors are given by $(X, Y = V, A)$:

$$H_{\mu\nu}^{XY} := -\mathrm{Tr}\left\{\left(\not{p}_f + m_f\right)\left(T_\mu^{X(1)} + T_\mu^{X(2)}\right)\left(\not{p}_{f'} - m_{f'}\right)\left(\overline{T_\nu^{Y(1)}} + \overline{T_\nu^{Y(2)}}\right)\right\}, \tag{65}$$

with the amplitudes ($X_\mu = \gamma_\mu, \gamma_\mu\gamma_5$ for $X = V, A$):

$$T_\mu^{X(1)} = \overline{u(p_f)}\left\{ X_\mu \frac{\not p - \not p_{f'} + m_{f'}}{(p - p_{f'})^2 - m_{f'}^2}\gamma_\alpha \right\} v(p_{f'})\varepsilon_\alpha(p),$$

$$T_\mu^{X(2)} = \overline{u(p_f)}\left\{ \gamma_\alpha \frac{\not p_f - \not p + m_f}{(p_f - p)^2 - m_f^2} X_\mu \right\} v(p_{f'})\varepsilon_\alpha(p). \tag{66}$$

We use

$$\sum_{\text{spins}} u(p_f)\overline{u(p_f)} = \not p_f + m_f \tag{67}$$

which is consistent with our phase space measure

$$\mathrm{d}\tilde{p}_f \equiv \frac{\mathrm{d}^3 p_f}{2E_f(2\pi)^3}. \tag{68}$$

The most general expansion of the (parity even) hadron tensors $H^1_{\mu\nu}$ and $H^2_{\mu\nu}$ is given by ($i = 1, 2$):

$$H^i_{\mu\nu} = \sum_{k=1}^{10} H_k^{(i)} B_{\mu\nu}^{(k)}, \tag{69}$$

where

$$\begin{aligned}
B_{\mu\nu}^{(1)} &:= g_{\mu\nu}, \\
B_{\mu\nu}^{(2)} &:= \frac{p_\mu p_\nu}{y s_{\mathrm{G}}}, \\
B_{\mu\nu}^{(3)} &:= \frac{q_\mu q_\nu}{y s_{\mathrm{G}}}, \\
B_{\mu\nu}^{(4)} &:= \frac{p_{f\mu} p_{f\nu}}{y s_{\mathrm{G}}}, \\
B_{\mu\nu}^{(5)} &:= \frac{p_\mu q_\nu + q_\mu p_\nu}{2 y s_{\mathrm{G}}}, \\
B_{\mu\nu}^{(6)} &:= \frac{p_\mu p_{f\nu} + p_{f\mu} p_\nu}{2 y s_{\mathrm{G}}}, \\
B_{\mu\nu}^{(7)} &:= \frac{q_\mu p_{f\nu} + p_{f\mu} q_\nu}{2 y s_{\mathrm{G}}}, \\
B_{\mu\nu}^{(8)} &:= \frac{p_\mu q_\nu - q_\mu p_\nu}{2 y s_{\mathrm{G}}}, \\
B_{\mu\nu}^{(9)} &:= \frac{p_\mu p_{f\nu} - p_{f\mu} p_\nu}{2 y s_{\mathrm{G}}}, \\
B_{\mu\nu}^{(10)} &:= \frac{q_\mu p_{f\nu} - p_{f\mu} q_\nu}{2 y s_{\mathrm{G}}}.
\end{aligned} \tag{70}$$

The analogous expansion of the two further (parity odd) hadron tensors $H^3_{\mu\nu}$ and $H^4_{\mu\nu}$ is ($i = 3,4$):

$$H^i_{\mu\nu} = \sum_{k=1}^{6} H^{(i)}_k A^{(k)}_{\mu\nu}, \tag{71}$$

where

$$A^{(1)}_{\mu\nu} := \frac{i}{yS_G}\varepsilon_{\mu\nu\rho\sigma}p^\rho q^\sigma,$$

$$A^{(2)}_{\mu\nu} := \frac{i}{yS_G}\varepsilon_{\mu\nu\rho\sigma}p^\rho p_f^\sigma,$$

$$A^{(3)}_{\mu\nu} := \frac{i}{yS_G}\varepsilon_{\mu\nu\rho\sigma}q^\rho p_f^\sigma,$$

$$A^{(4)}_{\mu\nu} := \frac{i}{yS_G}\left(p_{f\mu}F_\nu + p_{f\nu}F_\mu\right),$$

$$A^{(5)}_{\mu\nu} := \frac{i}{yS_G}\left(p_\mu F_\nu + p_\nu F_\mu\right),$$

$$A^{(6)}_{\mu\nu} := \frac{i}{yS_G}\left(q_\mu F_\nu + q_\nu F_\mu\right), \tag{72}$$

and $F_\mu = \varepsilon_{\mu\nu\rho\sigma}p^\nu q^\rho p_f^\sigma$.

However, we are only interested in the $O(\alpha_s)$ cross section. Then not all of the terms in (69) and (71) contribute to the cross section. First note that the (tree) hadron tensors are real. Thus there is no contribution to $B^{(i)}_{\mu\nu}$ for $i = 8,9,10$ and to $A^{(i)}_{\mu\nu}$ for $i = 4,5,6$. Further, since we neglect the lepton masses, all terms proportional to q_μ and q_ν in (69) can be dropped when contracting with the lepton tensor using

$$q^\mu L_{\mu\nu} = 0 = q^\nu L_{\mu\nu}. \tag{73}$$

Also we find that $H^3_{\mu\nu}$ is identically zero. For the remaining contributing terms one

obtains ($H_i^{(j)} \equiv H_i^{(j)}(x_G, z; y, s_G)$)*:

$$H_1^{(1)} = \frac{4}{z(1-z)}\{2z(1-z)+2x_G(1-x_G)-1\} + \frac{4}{z^2(1-z)^2}$$
$$\times\{-m_+^4+m_+^2m_-^2(2z-1)+m_+^2(2z(z-1)(x_G-1)-x_G)$$
$$+m_-^2x_G(2z-1)\},$$

$$H_2^{(1)} = 16\left\{\frac{x_G}{z(1-z)}+\frac{m_+^2+(1-z)m_-^2}{z^2(1-z)}\right\},$$

$$H_4^{(1)} = \frac{32x_G}{z(1-z)}+\frac{16}{z^2(1-z)^2}\{m_+^2+(1-2z)m_-^2\},$$

$$H_6^{(1)} = -\frac{32x_G}{z(1-z)}-\frac{32}{z^2(1-z)}\{m_+^2+(1-z)m_-^2\},$$

$$H_1^{(2)} = -\frac{16m_0(1-x_G)}{z(1-z)}+\frac{8m_0}{z^2(1-z)^2}\{m_+^2+(1-2z)m_-^2\},$$

$$H_2^{(2)} = -\frac{32m_0}{z(1-z)},$$

$$H_4^{(2)} = 0,$$

$$H_6^{(2)} = 0,$$

$$H_1^{(4)} = -\frac{8}{z^2(1-z)}\{-z^2+zx_G+m_+^2+(1-z)m_-^2\},$$

$$H_2^{(4)} = 0,$$

$$H_3^{(4)} = 8\frac{1-2x_G}{z(1-z)}-8\frac{m_+^2+(1-2z)m_-^2}{z^2(1-z)^2}. \qquad (74)$$

* Note that the two p.c. hadron tensors are not gauge invariant, only $q^\mu H_{\mu\nu}^4 = 0$.

Here we have defined:

$$m_+^2 = \frac{m_f^2 + m_{f'}^2}{y s_G},$$

$$m_-^2 = \frac{m_f^2 - m_{f'}^2}{y s_G},$$

$$m_0 = \frac{m_f m_{f'}}{y s_G}. \tag{75}$$

Let us now perform the contractions of the lepton tensors with the hadron tensors $L_i^{\mu\nu} H_{\mu\nu}^j$ $(i = 1,2;\ j = 1,2,4)$. Since to $O(\alpha^2 \alpha_s)$ $L_1^{\mu\nu}$, $H_{\mu\nu}^1$ and $H_{\mu\nu}^2$ are symmetric under the exchange $\mu \leftrightarrow \nu$ whereas $L_4^{\mu\nu}$ and $H_{\mu\nu}^4$ are antisymmetric (under this exchange), only the following contractions contribute $(i = 1,2)$:

$$\begin{aligned}\frac{y}{2s_G} L_1^{\mu\nu} H_{\mu\nu}^i = {} & x_G y^2 G_1^{(i)}(x_G, z; y, s_G) + (1-y) G_2^{(i)}(x_G, z; y, s_G) \\ & + (2-y)\sqrt{1-y}\cos\Phi\, G_A^{(i)}(x_G, z; y, s_G) \\ & + 2x_G(1-y)\cos 2\Phi\, G_B^{(i)}(x_G, z; y, s_G)\end{aligned} \tag{76}$$

and

$$\frac{y}{2s_G} L_4^{\mu\nu} H_{\mu\nu}^4 = x_G y(2-y) G_3(x_G, z; y, s_G) + 2y\sqrt{1-y}\cos\Phi\, G_C(x_G, z; y, s_G). \tag{77}$$

The (partonic) structure functions $G_l^{(i)} \equiv G_l^{(i)}(x_g, z; y, s_G)$ are given by:

$$\begin{aligned}
G_1^{(1)} &= -2H_1^{(1)} + f(x_G, z; y, s_G) H_4^{(1)}, \\
G_2^{(1)} &= 2x_G f(x_G, z; y, s_G) H_4^{(1)} + H_2^{(1)} + g(x_G, z; y, s_G) \\
&\quad \times \left(H_6^{(1)} + g(x_G, z; y, s_G) H_4^{(1)}\right), \\
G_A^{(1)} &= \sqrt{x_G f(x_G, z; y, s_G)}\left(H_6^{(1)} + 2g(x_G, z; y, s_G) H_4^{(1)}\right), \\
G_B^{(1)} &= f(x_G, z; y, s_G) H_4^{(1)}, \\
G_1^{(2)} &= -2H_1^{(2)}, \\
G_2^{(2)} &= H_2^{(2)}, \\
G_A^{(2)} &= 0, \\
G_B^{(2)} &= 0, \\
G_3 &= H_1^{(4)} + zH_2^{(4)} - g(x_G, z; y, s_G) H_3^{(4)}, \\
G_C &= \sqrt{x_G f(x_G, z; y, s_G)}\left(H_2^{(4)} - 2x_G H_3^{(4)}\right).
\end{aligned} \tag{78}$$

Here we have defined

$$f(x_G, z; y, s_G) := (1-x_G)z(1-z) + \frac{z\left(m_f^2 - m_{f'}^2\right) - m_f^2}{y s_G},$$

$$g(x_G, z; y, s_G) := (1-x_G)(1-z) + x_G z + m_-^2 . \tag{79}$$

The Φ-independent structure functions are given explicitly by:

$$\begin{aligned}
G_1^{(1)} = {} & \frac{8}{z(1-z)}\Big\{\left(x_G^2 + (1-x_G)^2\right)\left(z^2 + (1-z)^2\right) \\
& + 2\left((1-2z)(1-2x_G)m_-^2 - x_G m_+^2\right)\Big\} \\
& + \frac{8}{z^2(1-z)^2}\left\{\left(x_G - m_+^2\right)(1-2z)m_-^2 + (4z - 4z^2 - 1)m_-^4 + x_G m_+^2\right\}, \\
G_2^{(1)} = {} & 2x_G\left[G_1^{(1)} + 64x_G(1-x_G)\right] \\
& - \frac{16}{z^2(1-z)^2}\left\{(1-2z)m_-^6 + m_-^4 m_+^2 + 3x_G(2z-1)m_-^2 m_+^2\right. \\
& \qquad - x_G m_+^4 \\
& \qquad - 4m_-^2(2z-1)z(z-1)x_G(2x_G-1) \\
& \qquad \left. - 2m_-^4\left(z(1-z)(1-5x_G) + x_G\right)\right\} \\
& + \frac{16m_+^2}{z(1-z)}\left(6x_G^2 - 2x_G - 1\right), \\
G_3 = {} & \frac{8}{z(1-z)}(2z-1)\left(2x_G^2 - 2x_G + 1\right) \\
& + \frac{\begin{array}{l} 8m_-^4(1-2z) + 8m_-^2 m_+^2 \\ + 8m_-^2\left(-6z^2x_G + 2z^2 + 6zx_G - 2z - x_G\right) + 8m_+^2 x_G(2z-1) \end{array}}{z^2(1-z)^2} .
\end{aligned} \tag{80}$$

Note that the partonic structure functions $G_i^{(l)}$ are still y-dependent as long as the quark masses are nonzero. The representations (76, 77) of the y-dependence are

thus not unique in the massive case. These decompositions were chosen to allow for a simple comparison with the usual (massless) results [14, 15].

References

[1] R.J. Cashmore et al. Phys. Rev. 122 (1985) 275;
G. Wolf, DESY 86-089 (1986)
[2] K.H. Streng, München preprint
[3] I. Hinchliffe, LBL-18572 (1984);
R. Rückl, DESY 87-021
[4] J. Babcock and D. Sivers, Phys. Rev. D18 (1978) 2301
[5] D.J. Gross and F. Wilczek, Phys. Rev. D9 (1974) 980;
H. Georgi and H.D. Politzer, Phys. Rev. D9 (1974) 416
[6] M. Glück, E. Hoffmann and E. Reya, Z. Phys. C13 (1982) 119
[7] M. Drees and K. Grassie, Z. Phys. C28 (1985) 451
[8] E. Gabrielli, Mod. Phys. Lett. A1 (1986) 465
[9] M. Glück and E. Reya, Phys. Lett. 83B (1979) 98;
L.M. Jones and H.W. Wyld, Phys. Rev. D17 (1978) 759
[10] E. Witten, Nucl. Phys. B104 (1976) 445;
M.A. Shifman, A.I. Vainshtein and V.I. Zakharov, Nucl. Phys. B136 (1978) 157;
J.P. Leveille and T. Weiler, Nucl. Phys. B147 (1979) 147
[11] M. Glück, R.M. Godbole and E. Reya, DO-TH 87/12 (1987)
[12] R. Eichler and Z. Kunszt, to be published
[13] R. Moore, Nucl. Phys. B191 (1981) 113
[14] R.D. Peccei and R. Rückl, Nucl. Phys. B162 (1980) 125
[15] A. Mendez, Nucl. Phys. B145 (1978) 199
[16] E. Byckling and K. Kajantie, Particle kinematics (Wiley, London)
[17] D.W. Duke and J.F. Owens, Phys. Rev. D30 (1984) 49
[18] E. Eichten, I. Hinchliffe, K. Lane and C. Quigg, Rev. Mod. Phys. 56 (1984) 579; (E) 58 (1986) 1065
[19] J. Engelen, S. de Jong and J. Vermaseren, private communication
[20] U. Baur and J.J. van der Bij, CERN-TH.4875/87 (1987)